TM-71-1011-1

TECHNICAL MEMORANDUM

A PHOTOMETRIC STUDY OF THE ECLIPSING BINARY STAR SYSTEM RU URSA MINORIS

Bellcomm

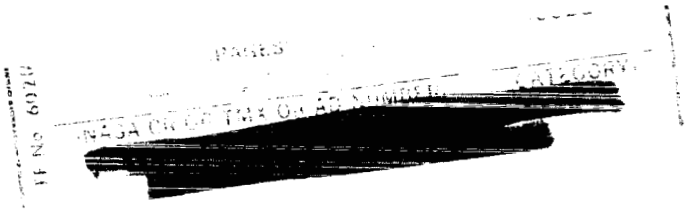

BELLCOMM, INC.
955 L'ENFANT PLAZA NORTH, S.W. WASHINGTON, D.C. 20024

COVER SHEET FOR TECHNICAL MEMORANDUM

TITLE- A Photometric Study of the Eclipsing Binary Star System RU Ursa Minoris

TM- 71-1011-1

DATE- February 8, 1971

FILING CASE NO(S)- 105-9

AUTHOR(S)- D. B. Wood

FILING SUBJECT(S)- Astronomy
(ASSIGNED BY AUTHOR(S)- Eclipsing Stars

ABSTRACT

Using only photometric data, the absolute elements of RU Ursa Minoris, a close eclipsing binary star, have been determined. The calculation is based on a computer model of eclipsing binary systems and on the following assumptions:

1) Relationship between stellar mass and distortion as determined by Chandrasekhar.

2) Applicability of the Stefan and Planck laws to stellar radiation.

3) Relationship between stellar mass and luminosity (the "mass-luminosity" law) for the primary star.

Normally, the physical properties of eclipsing binary stars are obtained through the combined results of photometry and spectroscopy. However, the unique properties of this system, combined with the above assumptions, allow the analysis to be performed without spectroscopic observations.

Both stars are apparently oversize for their mass and temperature. The dwarf primary star has a temperature of about 7200°K and fills its Roche limiting surface. The star has expanded to its maximum permissable size. The secondary star has a temperature on the order of 4000°K and its radius is similarly nearly at its Roche limit. The surfaces of the stars are separated by less than one solar radius.

SEE REVERSE SIDE FOR DISTRIBUTION LIST

DISTRIBUTION

COMPLETE MEMORANDUM TO

CORRESPONDENCE FILES:

OFFICIAL FILE COPY
plus one white copy for each additional case referenced

TECHNICAL LIBRARY (4)

NASA Headquarters

W. O. Armstrong/MTL
P. E. Culbertson/MT
C. J. Donlan/MD-T
E. W. Hall/MTG
H. Hall/MT-2
T. A. Keegan/MA-2
A. S. Lyman/MR
G. K. Oertel/SG
N. G. Roman/SG
J. W. Wild/MTE

Bellcomm, Inc.

A. P. Boysen, Jr.
F. El-Baz
K. R. Carpenter
C. L. Davis
D. R. Hagner
N. W. Hinners
D. P. Ling
H. S. London
K. E. Martersteck
J. Z. Menard
G. T. Orrok
F. N. Schmidt
J. W. Timko (2)
M. P. Wilson
Department 1013 Supervision
Department 1014 Supervision
Department 1015 Supervision
Division 102 Supervision
All Members, Dept. 1011, 2015
Central Files
Department 1024 File
Library

COVER SHEET ONLY TO

Bellcomm, Inc.

J. P. Downs
R. L. Wagner

Complete Memorandum To

GSFC

K. L. Hallam/613
S. Sobieski/613
A. B. Underhill/613

MSC

K. Henize/CB
Y. Kondo/TG4
T. L. Page/TG4

BELLCOMM, INC.
955 L'ENFANT PLAZA NORTH, S.W. WASHINGTON, D. C. 20024

SUBJECT: A Photometric Study of the Eclipsing Binary Star System RU Ursa Minoris
Case 105-9

DATE: February 8, 1971

FROM: D. B. Wood

TM: 71-1011-1

TECHNICAL MEMORANDUM

INTRODUCTION

Most of our information about the mass, radius and luminosity of stars comes from a special class of stars known as eclipsing binary stars. These star systems consist of two stars which orbit each other and, in particular, have an orbital plane which nearly aligns with the earth. Thus, as these stars revolve, each one is alternately eclipsed by the other, as seen from the earth.

For several years, I have been developing a computer model of such eclipsing binary systems. The details of this model will be reported in a later memorandum.* This model has a number of adjustable parameters, to account for the various photometric perturbations, such as tidal distortion and reflection, which occur when two stars are very close together (near surface-contact).

In order to debug the model, it has been subjected to a variety of test conditions. This memorandum reports on some interesting results obtained by applying this model, along with some additional calculations, to observational data obtained on a trip to Kitt Peak National Observatory.

The eclipsing system RU Ursa Minoris was observed during the spring of 1970 using the 16-inch telescope at Kitt Peak. Photoelectric observations were made with the Strömgren 4-color system**, and light curves were obtained in b and y. Strömgren has defined several special color indices using the 4-color filters. The b-y index is a "color", and is indicative of stellar temperature. The brighter the y magnitude, compared with b, the "redder" or cooler is the star. The indices m_1 and c_1 are measures of stellar metal content and luminosity.

---

*The model is described briefly in Reference 10.

**This photometric system consists of four interference filters, each with a bandpass of approximately 200 Å, with the following effective wavelengths: y filter, 5500 Å; b filter, 4700 Å; v filter, 4100 Å; u filter, 3450 Å.

The photoelectric observations of the variable star RU UMi were compared with observations of several comparison stars, which are assumed to be constant in brightness. The use of more than one comparison star helps to insure that a truly constant star is available for comparison with the variable star. The photometric properties of the comparison stars and of RU UMi at maximum light are shown in Table I. The column headed "Sp" refers to spectral type. Stars are classified, based on the appearance of their spectrum, by a letter designation. For historical, rather than logical, reasons this sequence of letter types is O, B, A, F, G, K, M. Type O stars are the hottest (over 30,000°K) and type M stars are the coolest (less than about 3000°K). Each class is sub-divided into ten parts, indicated by the digits 0 through 9. In addition, where it can be determined, spectra are further classified supergiant through dwarf by the addition of the Roman numerals I through V. These latter designations, called "luminosity class", were not intended to characterize physical size, but rather the absolute (i.e. intrinsic) luminosity. Fortuitously, supergiant stars are larger than dwarf stars.

By combining the observed times of primary (deeper) eclipse with older observations (taken from Reference 9) an up-to-date ephemeris for the variable star is obtained:

$$\text{JD Hel. Min} = 2440708.6848 + .52492605\ E.$$

JD Hel. Min. is the Julian Date of minimum light (as seen from the sun) at cycle E from the observed JD Hel. Min. of 2440708.6848. The period of this eclipsing star is .52492605 days. The (observed - computed) residuals of this emphemeris compared to all known observed times of minimum are shown in Table II.

Since the variable star is quite faint for 4-color photometry using a 16-inch telescope, the observed data were smoothed by forming means of several observations. These "normal points" are tabulated in Table III and exhibited in Figures 1 and 2. The ordinate is phase, that is time expressed in units of period, measured from primary eclipse. The RMS error of the normal points is about ± 0.01 magnitude.

The Strömgren indices for RU UMi, for several random phases, are shown in Table IV. Insufficient data is available to establish the reality of the apparent variation in m_1 and c_1. The variation in b-y is real, as confirmed by analysis of all the data of Table III. Primary eclipse (phase 0) is redder than secondary eclipse (phase .5), hence the secondary star, which contributes relatively more light at primary eclipse, is the cooler star.

Analysis

In the ensuing analysis, the following parameters are used:

- a — semi-major axis of the primary (more luminous) star (assumed ellipsoidal)
- b — semi-axis of this star, in the orbital plane, perpendicular to a
- c — semi-axis of this star perpendicular to the orbital plane
- a_o — the "unperturbed" radius of this star, i.e., the radius of a sphere of comparable volume to the ellipsoid
- q — the mass ratio (mass of the secondary star divided by mass of the primary star)
- a', b', c', a_o', q' — Identical quantities for the secondary star - note that $q' \equiv 1/q$
- L — stellar luminosity
- $L_\odot$ — solar luminosity
- $R_\odot$ — solar radius
- T — effective stellar temperature
- $T_\odot$ — effective solar temperature
- m — stellar mass
- $m_\odot$ — solar mass

A semi-major axis of stellar orbit

A_o semi-major axis of earth's orbit

P period of stellar orbit

M absolute stellar magnitude

$M_\odot$ absolute solar magnitude

j surface brightness ratio of the two stars (seondary/primary)

u limb darkening coefficient, which measures the rate that surface intensity decreases to the limb of a star

F radiant flux

The light curves (Figures 1 and 2) were fit by the computer model, using a trial-and-error procedure. The blue curve was fit first, and then the yellow curve was fit, but constrained to have the same orbital inclination and axes as the blue solution. The details of the final fit are shown in Figures 3 and 4. In these figures, the descending and ascending branches of the light curve in eclipse have been folded over, which forces a symmetric eclipse profile. Secondary eclipse is displayed below primary eclipse for convenience. The fit is not necessarily unique, but is obviously satisfactory. The model parameters thus obtained for the two stars are listed in Table V.

Gravity brightening is a term applied to describe the dependence of stellar surface brightness upon the local surface gravity. The equator of an oblate star is cooler, hence of lower surface brightness, than is the pole, because surface gravity is lower on the equator. The value of the gravity brightening coefficient used in this model fit is constrained to be consistent with that theoretically calculated from radiative transfer (Reference 5). Some recent work, however, contradicts this. The dependence upon surface gravity may be much stronger (Reference 6) or may be much weaker (Reference 7). The ellipticity of the stars, as determined by the model fit to the light curve, depends upon the gravity brightening coefficient. An ellipsoidal star with strong gravity brightening is effectively (in terms of the viewed photometric effect) more elliptical.

From the work of Chandrasekhar (Reference 2) the axes of an ellipsoidal star are relatable to the mass ratio:

$$\left.\begin{aligned} \frac{a}{A} &= \frac{a_o}{A}\left[1 + \frac{1}{6}(1+7q)\Delta_2\left(\frac{a_o}{A}\right)^3\right] \\ \frac{b}{A} &= \frac{a_o}{A}\left[1 + \frac{1}{6}(1-2q)\Delta_2\left(\frac{a_o}{A}\right)^3\right] \\ \frac{c}{A} &= \frac{a_o}{A}\left[1 - \frac{1}{3}(1+\frac{5}{2}q)\Delta_2\left(\frac{a_o}{A}\right)^3\right] \end{aligned}\right\} \qquad (1)$$

where Δ_2 is a parameter related to the degree of central mass concentration. It can be taken here to be unity. We can write three identical equations for a'/A, b'/A and c'/A. The fit to the light curve easily establishes the ellipticity and major axis of the brighter star and the ratio, a'/a, of the major axes of the two stars; hence we have a/A, a'/A and b/A. Since q'=1/q, we are left with six equations in the six unknowns b'/A, c/A, c'/A, a_o/A, a_o'/A and q.

The light curve solution shows that the primary star provides about 98% of the system luminosity. Thus its ellipticity alone is responsible for the out-of-eclipse light variation; in fact, its ellipticity is responsible for almost all the light variation in secondary eclipse. This "eclipse", due to viewing the distorted star end-on, is about 0.2 mag. deep. If the secondary star were to be totally eclipsed, the light would be reduced by only about 0.02 mag.

THE PRIMARY STAR

The spectral type of RU UMi has been determined to be A2 by one observer (Reference 3) and F5 by another (Reference 8). The photometric indices in Table I indicate a spectral type of A9-FO IV-V. We can assume the primary star to be of spectral type FOV, with an effective surface temperature of 7200°K, and calculate the mass, radius, and luminosity using the three familiar relationships:

$$\left(\frac{L}{L_\odot}\right) = \left(\frac{a_o}{R_\odot}\right)^2 \left(\frac{T}{T_\odot}\right)^4 \qquad \text{(From Stefan's Law)} \qquad (2)$$

$$\frac{(1+q)m}{m_\odot} P^2 = \left(\frac{A}{A_o}\right)^3 \qquad \text{(From Kepler's Law)} \qquad (3)$$

$$\log \left(\frac{L}{L_\odot}\right) = 3.3 \log \left(\frac{m}{m_\odot}\right) \qquad \text{(Mass-luminosity Law).} \qquad (4)$$

For our calculations, it is convenient to rewrite these equations in logarithmic form. In Equation (2) we introduce the absolute bolometric magnitude, M_B, ($M_{B\odot} = 4.72$) and write*

$$M_B = 4.72 - 5 \log \frac{A}{R_\odot} - 5 \log \frac{a_o}{A} - 10 \log \frac{T}{T_\odot} \quad . \qquad (5)$$

Introducing the A.U. in units of $R_\odot$ for A_o and allowing P to be expressed in days, Equation (3) becomes

$$\log \frac{m}{m_\odot} + \log (1+q) + 2 \log P = 3 \log \frac{A}{R_\odot} - 1.87 \quad . \qquad (6)$$

Equation (4), which was taken from Reference 1, is conveniently written

$$\log \frac{m}{m_\odot} = 0.57 - 0.121 M_B \quad . \qquad (7)$$

From the light curve solution we find q and a_o/A. The photometric observations have also allowed determination of P and T. The effective temperature of the sun, $T_\odot$, is 5800°K. Thus Equations (5), (6) and (7) are three equations in the three unknowns M_B, $A/R_\odot$, and $m/m_\odot$. For the values of q, a_o/A, P and T which have been determined, we find

---

*The relationship between magnitude and luminosity is $M_1 - M_2 = -\frac{5}{2} \log \frac{L_1}{L_2}$.

$$A/R_{\odot} = 3.7 \pm .1$$

$$m/m_{\odot} = 1.7 \pm .2$$

$$M_B = 2.9 \pm .3$$

The axes of the primary star are thus

$$a_o/R_{\odot} = 1.7 \pm .1$$

$$a/R_{\odot} = 1.8 \pm .1$$

$$b/R_{\odot} = 1.7 \pm .1$$

$$c/R_{\odot} = 1.6 \pm .1$$

The quoted probable errors are based upon an estimated uncertainty in a_o/A of $\pm$ .01 and in q of $\pm$ .1. The uncertainty in T, estimated to be less than $\pm$200°K, is not significant.

THE SECONDARY STAR

As was pointed out above, the secondary star is hardly detectable photoelectrically; most of secondary eclipse is not due to the light loss of the eclipsed secondary star. In blue light, the secondary has a surface brightness of about 0.02 that of the primary. In yellow, the factor is up to about 0.07.

If the assumption is made that the radiation of both the primary and secondary components may be approximated by the Planck function (over the pass bands of the b and y filters) then the temperature of the secondary component can be estimated. In Reference 1, the black body flux in units of the flux at maximum ($F_\nu/F_{\nu m}$) is tabulated as a function of λT, where

$$F_{\nu m} = 5.96 \times 10^{-16} T^3 \quad . \qquad (8)$$

Figure 5 shows a plot of this blackbody function $F_\nu/F_{\nu m}$ vs λT over the range of interest. The ordinate, λT, is expressed in cm-deg. The secondary star radiates j times as much energy per unit area as does the primary, so we may express the flux of the secondary, $F_\nu(s)$, in terms of the flux of the primary, $F_\nu(P)$;

$$\frac{F_\nu(s)}{F_{\nu m}(s)} = \frac{j\, F_\nu(P)}{F_{\nu m}(s)} = j\, \frac{F_\nu(P)}{F_{\nu m}(P)}\, \frac{F_{\nu m}(P)}{F_{\nu m}(s)} \quad . \tag{9}$$

$[F_\nu(P)/F_{\nu m}(P)]$ is the value for the primary star. From Equation (8), the ratio $[F_{\nu m}(P)/F_{\nu m}(s)]$ is just $[T(P)/T(s)]^3$. The surface intensity ratio, j, is given in Table V. Thus for the blue (λ = 4700 Å) observations and for the yellow (λ = 5500 Å) observations, independent estimates of T(s) may be made by determining the ordinate where $[F_\nu(s)/F_{\nu m}(s)]$, calculated from Equation (9), intersects the blackbody curve of Figure 5. Curves calculated for a variety of values of j for each color are shown. In Table VI the temperatures are shown as calculated from the value of λT at the intersections in Figure 5. The most consistent set is for $j_y = 0.05$ and $j_b = 0.03$, indicating a temperature of 3950°K. The range of j which is consistent with the light curve solution introduces a temperature uncertainty of about ±300°K. This temperature and uncertainty would indicate a spectral type of K3V to K7V.

The resulting ratio of surface intensities, j_b/j_y, can be used to calculate the Δ(b-y) color between the two components:

$$\Delta(b-y) = -\frac{5}{2} \log (j_b/j_y) \quad . \tag{10}$$

For $j_b = .03$ and $j_y = .05$, we find $\Delta(b-y) = .55$; thus the color of the secondary star is (b-y) = 0.75, which corresponds to a spectral type of K6-7V. This is consistent with the K3-7V determined above.

The computer model used defines j at the sub-earth point at quadrature, when the two stars are seen broadside. Reflection effects are confined primarily to the sub-stellar regions, 90° away. Hence this calculation of the temperature and spectral type of the secondary star represents its values at the end of the b-axis, where there is very little perturbation from reflection. However, in order to obtain the absolute magnitude difference between the two stars, we must be careful how we obtain the total integrated luminosity from each star. The relative luminosity in Table V includes reflected light, so that part of the light of the secondary star is light of the primary which is reflected.

If we assume each star to be a sphere (of the unperturbed radius), then the magnitude difference between the two stars can be expressed by

$$\Delta M = -\frac{5}{2} \log [L(s)/L(P)] = -\frac{5}{2} \log \{j[a_o(s)/a_o(P)]^2\}. \quad (11)$$

Thus in yellow light, $\Delta M_y = 4.5$ mag. In blue light, $\Delta M_b = 5.1$ mag; however, since we established that $\Delta(b-y) = 0.75$, this yields $\Delta M_y = 4.3$ mag. At 4000°K, the bolometric correction is +0.6; so the absolute bolometric magnitude difference, ΔM_B is approximately 5.0 mag. Consequently, the absolute bolometric magnitude of the secondary is 7.9 mag., but the uncertainty is on the order of $\pm$.75 mag.

DISCUSSION

In Table VII the resulting calculated absolute properties of the primary and secondary stars are compared with standard values. YY Geminorum is a well-known eclipsing system of spectral type M1. In general, the calculated parameters for both components of RU UMi are consistent. However both stars are oversize for their mass. Table VIII compares the axes of these stars with the dimensions of the Roche limiting surface for q = .3 and q = .4 (Reference 5). In Figure 6 we see how this system would appear to a nearby observer. This scale drawing shows that the stars are separated by less than one solar radius. The outer dashed boundary is the Roche limiting surface. The circles show the sizes of normal stars of the same temperature and mass. These stars are very nearly at their Roche limits. RU UMi may be a "contact" system, similar to the class of stars known by their prototype, W Ursa Majoris. If this is true, this is a unique system, for no W UMa type systems possess such cool, faint secondary components.

Because of the recent evidence of weaker gravity brightening (References 4 and 7), a model was constructed with gravity coefficients of -1.0 for the primary and -2.0 for the secondary (as opposed to the values listed in Table V). To obtain the same photometric distortion in the light curve, the primary star must be more distorted; thus the mass ratio must be larger [see Equations (1)]. In this case we find q = .6, $A/R_\odot = 4.0$, $m/m_\odot = 2.2$, $M_B = 2.1$, and $a/R_\odot = 2.0$. For the secondary star, $m/m_\odot = 1.3$, $M_B = 7.1$, $a/R_\odot = 1.0$. These values are not consistent with the color data, so the stronger gravity dependence for gravity brightening seems more reasonable.

Based on the photometric data, the spectroscopic orbit should show an amplitude, K, of 350 km/sec, and a mass function, f(m), of approximately 0.09.

D B Wood

1011-DBW-ulg

D. B. Wood

REFERENCES

1. Allen, C. W. 1963, Astrophysical Quantities (Athlone Press, London).

2. Chandrasekhar, M. S. 1933, M.N.R.A.S. 93, 462.

3. Götz, W. and Wenzel, W. 1964, Mitt. über verändliche Sterne, 2, 85.

4. Hill, G. and Hutchings, J. B. 1970, Ap.J., 162, 265.

5. Kopal, Z. 1959, Close Binary Systems (Wiley and Sons, N. Y.).

6. Kopal, Z. 1968, Ap. and Sp. Sci. 2, 23.

7. Lucy, L. 1967, Zeit.f.Ap. 65, 89.

8. MacDonald, D. D. 1964, Publ. Leander McCormick Obs., 12.

9. Strohmeier, W. and Knigge, R. 1960, Bamberg Veröffent. Remeis, 5.

10. Wood, D. B. 1969, Bull. A.A.S. 1, 267.

Table I

Photometric Data on Comparison Stars

Star	Sp	m_v	b-y	m_1	c_1
RU UMi	FO	10.03	.195	.136	.712
+70 753*	G5	8.58	.588	.350	.444
+70 748*	F5	8.25	.291	.168	.388
+70 749*	--	10.13	.422	--	--

*Bonner Durchmusterung catalog designation.
RU UMi is +70 751 in this catalog.

Table II

Times of Minimum of RU UMi

JD Hel.	Epoch	O-C	Source
242 6456.397	-27151	-.021	Strohmeier and Knigge
6509.449	-27050	+.014	"
6744.607	-26602	+.005	"
7133.563	-25861	-.009	"
8248.505	-23737	-.010	"
8310.454	-23619	-.002	"
8690.492	-22895	-.011	"
8751.407	-22779	+.013	"
9014.387	-22278	+.005	"
9341.422	-21655	+.011	"
9373.419	-21594	-.013	"
243 6611.631	- 7805	-.006	"
6612.675	- 7803	-.012	"
6630.565	- 7769	+.031	"
6661.497	- 7710	-.008	"
6662.554	- 7708	-.001	"
244 0707.6352	- 2	+.0002	Wood
0708.6853	0	+.0005	"
0710.7841	4	-.0004	"
0711.8340	6	-.0004	"

Table III

RU UMi Yellow Observations

Phase	Δy	n	Phase	Δy	n	Phase	Δy	n
.0021	2.127	3	.4276	1.606	4	.9564	1.930	3
.0044	2.093	4	.4380	1.622	3	.9605	1.956	4
.0078	2.090	2	.4485	1.644	2	.9666	1.985	3
.0113	2.127	3	.4624	1.656	2	.9702	2.002	3
.0128	2.125	3	.4720	1.663	3	.9738	2.048	2
.0172	2.124	2	.4796	1.643	3	.9764	2.070	3
.0216	2.093	5	.4856	1.656	2	.9802	2.076	2
.0262	2.097	2	.4906	1.666	2	.9840	2.090	3
.0278	2.031	2	.4984	1.662	2	.9891	2.103	3
.0315	2.032	3	.5082	1.643	3	.9923	2.087	3
.0362	1.975	5	.5172	1.662	2	.9959	2.108	2
.0382	1.990	2	.5248	1.653	4	.9991	2.097	3
.0423	1.966	3	.5549	1.653	3			
.0446	1.942	3	.5652	1.610	3			
.0471	1.917	4	.5794	1.578	2			
.0522	1.859	3	.5864	1.608	2			
.0572	1.827	3	.5960	1.583	3			
.0604	1.854	2	.6058	1.579	2			
.0636	1.830	2	.6300	1.554	2			
.0668	1.796	3	.6362	1.523	2			
.0708	1.732	1	.6434	1.530	2			
.0763	1.712	1	.6488	1.531	3			
.0843	1.684	2	.6766	1.532	2			
.0962	1.619	4	.6814	1.474	2			
.1003	1.610	2	.6902	1.508	3			
.1040	1.602	2	.6960	1.486	2			
.1099	1.583	3	.7257	1.448	3			
.1151	1.626	5	.7361	1.455	2			
.1346	1.519	1	.7475	1.470	2			
.1442	1.516	2	.7558	1.472	2			
.1543	1.509	2	.7592	1.448	2			
.1662	1.493	3	.7674	1.439	5			
.1754	1.475	3	.7904	1.498	2			
.1856	1.483	3	.8002	1.475	2			
.2034	1.469	3	.8060	1.454	2			
.3502	1.507	2	.8139	1.498	2			
.3582	1.480	2	.8251	1.454	2			
.3656	1.512	3	.9100	1.664	2			
.3736	1.548	3	.9230	1.726	2			
.3776	1.533	3	.9328	1.762	2			
.3865	1.537	3	.9404	1.814	3			
.3997	1.549	3	.9478	1.891	3			
.4083	1.578	3	.9521	1.945	3			
.4188	1.584	3						

Table III - Continued

RU UMi Blue Observations

Phase	Δb	n	Phase	Δb	n	Phase	Δb	n
.0027	1.710	3	.4636	1.217	2	.9585	1.536	2
.0049	1.706	3	.4729	1.234	3	.9620	1.574	3
.0078	1.715	3	.4805	1.230	3	.9664	1.573	2
.0119	1.700	3	.4865	1.233	2	.9700	1.583	3
.0136	1.701	3	.4918	1.242	2	.9730	1.657	2
.0189	1.719	3	.5012	1.226	3	.9763	1.658	3
.0231	1.684	4	.5115	1.212	2	.9788	1.688	2
.0281	1.656	4	.5184	1.234	2	.9830	1.678	2
.0319	1.593	3	.5242	1.219	3	.9851	1.687	2
.0365	1.554	5	.5306	1.237	1	.9899	1.705	3
.0390	1.572	2	.5558	1.222	2	.9930	1.693	3
.0439	1.538	3	.5663	1.219	2	.9968	1.710	2
.0473	1.509	5	.5802	1.176	2	.9999	1.720	3
.0529	1.471	3	.5870	1.158	2			
.0577	1.436	2	.5948	1.161	2			
.0600	1.426	2	.6046	1.152	3			
.0636	1.393	3	.6306	1.125	2			
.0687	1.370	4	.6370	1.137	2			
.0798	1.296	2	.6428	1.110	2			
.0916	1.230	2	.6495	1.121	3			
.0972	1.202	3	.6775	1.096	2			
.1030	1.195	4	.6822	1.076	2			
.1107	1.172	3	.6900	1.097	2			
.1145	1.182	3	.6971	1.090	2			
.1180	1.177	2	.7264	1.041	3			
.1355	1.137	1	.7372	1.090	2			
.1452	1.108	2	.7493	1.062	2			
.1556	1.088	2	.7566	1.058	2			
.1666	1.084	2	.7598	1.037	2			
.1770	1.046	2	.7655	1.046	1			
.1878	1.062	2	.7716	1.049	2			
.2036	1.056	2	.7914	1.089	2			
.3511	1.082	2	.8009	1.056	2			
.3591	1.120	2	.8068	1.064	2			
.3663	1.115	3	.8146	1.096	2			
.3728	1.124	1	.8258	1.031	2			
.3872	1.134	2	.9112	1.250	2			
.4005	1.146	3	.9217	1.286	1			
.4090	1.167	3	.9261	1.352	1			
.4192	1.185	2	.9334	1.370	2			
.4258	1.190	2	.9412	1.398	3			
.4308	1.204	2	.9484	1.457	3			
.4384	1.208	3	.9516	1.476	2			
.4496	1.201	2	.9570	1.500	2			

Table IV

Strömgren Indices as a Function of Phase

Phase	b-y	m_1	c_1
.025	.193	.22	.60
.205	.184	.16	.72
.445	.186	.20	.70
.505	.180	.22	.72
.555	.174	.22	.71
.570	.175	.16	.72
.730	.183	.11	.70
.945	.198	.16	.70

Table V

Photometric Orbital Elements for RU UMi

inclination 83°.0		
mass ratio, q .35		
	primary	secondary
unperturbed sphere radius a_o/A	.45	.25
semi-axes		
a/A	.480	.271
b/A	.457	.252
c/A	.429	.244
yellow light curve		
limb darkening, u	.89	.9*
gravity brightening†	-4.5	-6.5*
reflection albedo	.5	.5
luminosity, L	.971	.029
relative lum., L(s)/L(P)	.030	
surface intensity ratio, j	.070	
blue light curve		
limb darkening, u	.89	1.0*
gravity brightening†	-4.6	-7.5*
reflection albedo	.33	.33
luminosity, L	.988	.012
relative lum., L(s)/L(P)	.012	
surface intensity ratio, j	.020	

*Assumed values, appropriate †Equivalent to -b as defined by Kopal for very cool star

Table VI

Temperature Estimates for RU UMi Secondary

Yellow (λ = 5500Å)		Blue (λ = 4700Å)	
j	T (°K)	j	T (°K)
.05	3940	.01	3570
.06	4060	.02	3770
.07	4160	.03	3960
.08	4270		

Table VII

Comparison of the Absolute Elements of

the Components of RU UMi with Standard Stars

	RU UMi A	FOV	RU UMi B	K5V	YY Gem
Abs Bol Mag	2.9 ± .3	2.7	7.9 ± .8	6.8	7.7
T_e(K°)	7200 ± 200	7200	4000 ± 300	4000	3600
Mass (⊙)	1.7 ± .2	1.78	.6 ± .1	.69	.64
Radius (⊙)	1.7 ± .1	1.35	.9 ± .1	.74	.62

Table VIII

Comparison of the Axes of the Components

of RU UMi with the Roche Model

	RU UMi	Roche Model	
		q = .3	q = .4
a_o	.47	.48	.46
b	.46	.49	.46
c	.43	.45	.43
a'_o	.25	.28	.30
b'	.25	.27	.29
c'	.24	.26	.28

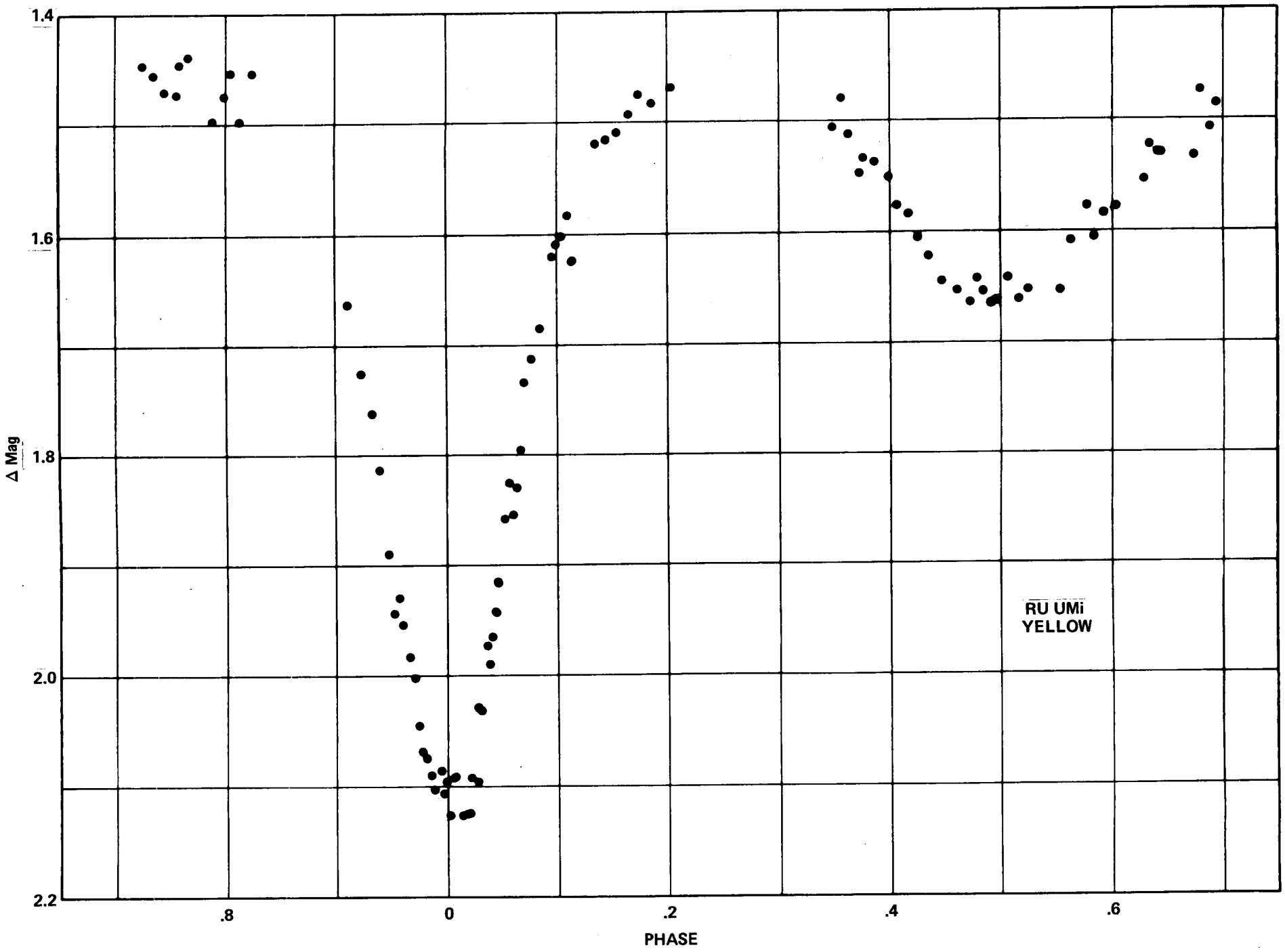

FIGURE 1 - YELLOW LIGHT CURVE FOR RU UMi

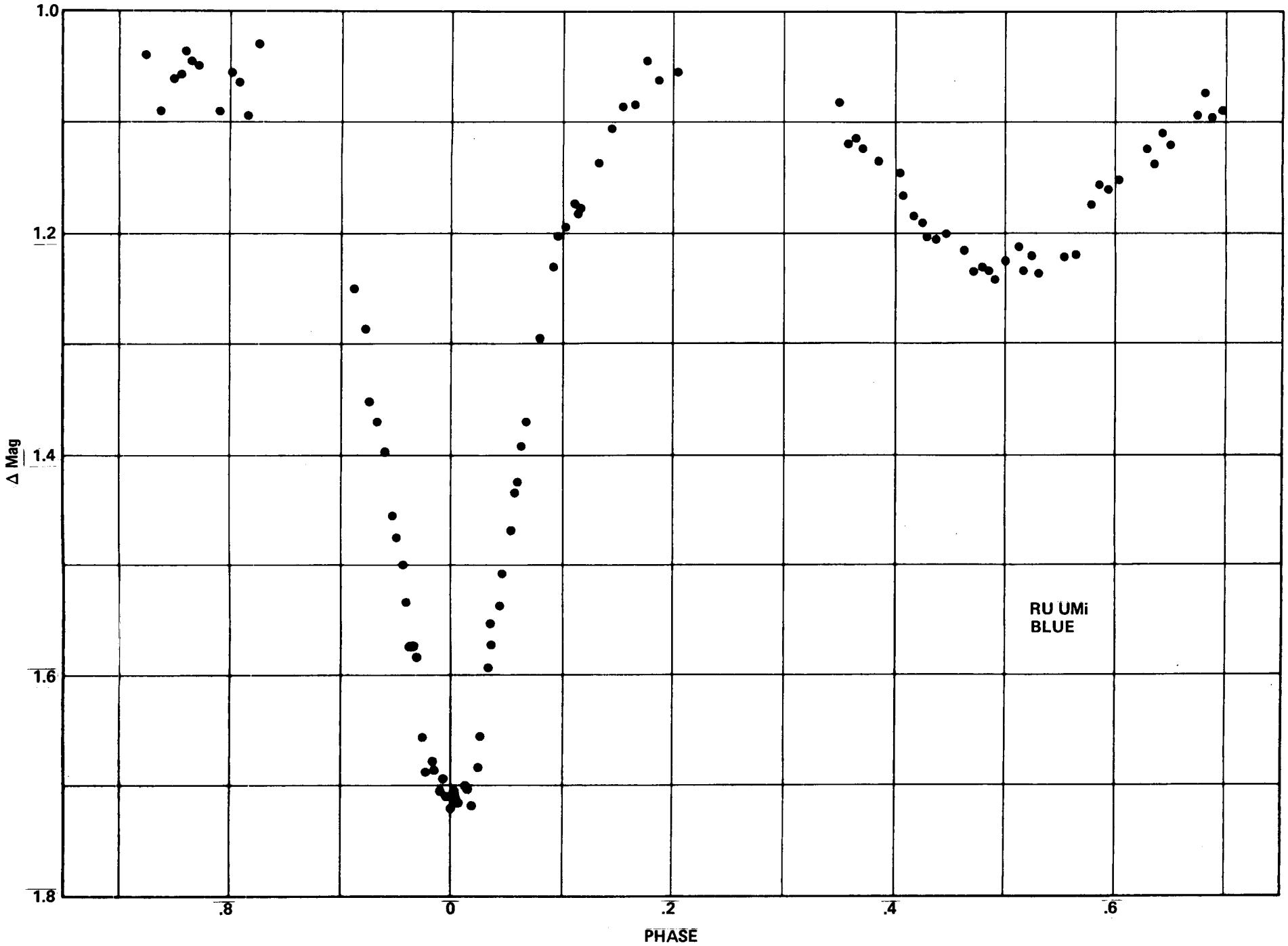

FIGURE 2 - BLUE LIGHT CURVE FOR RU UMi

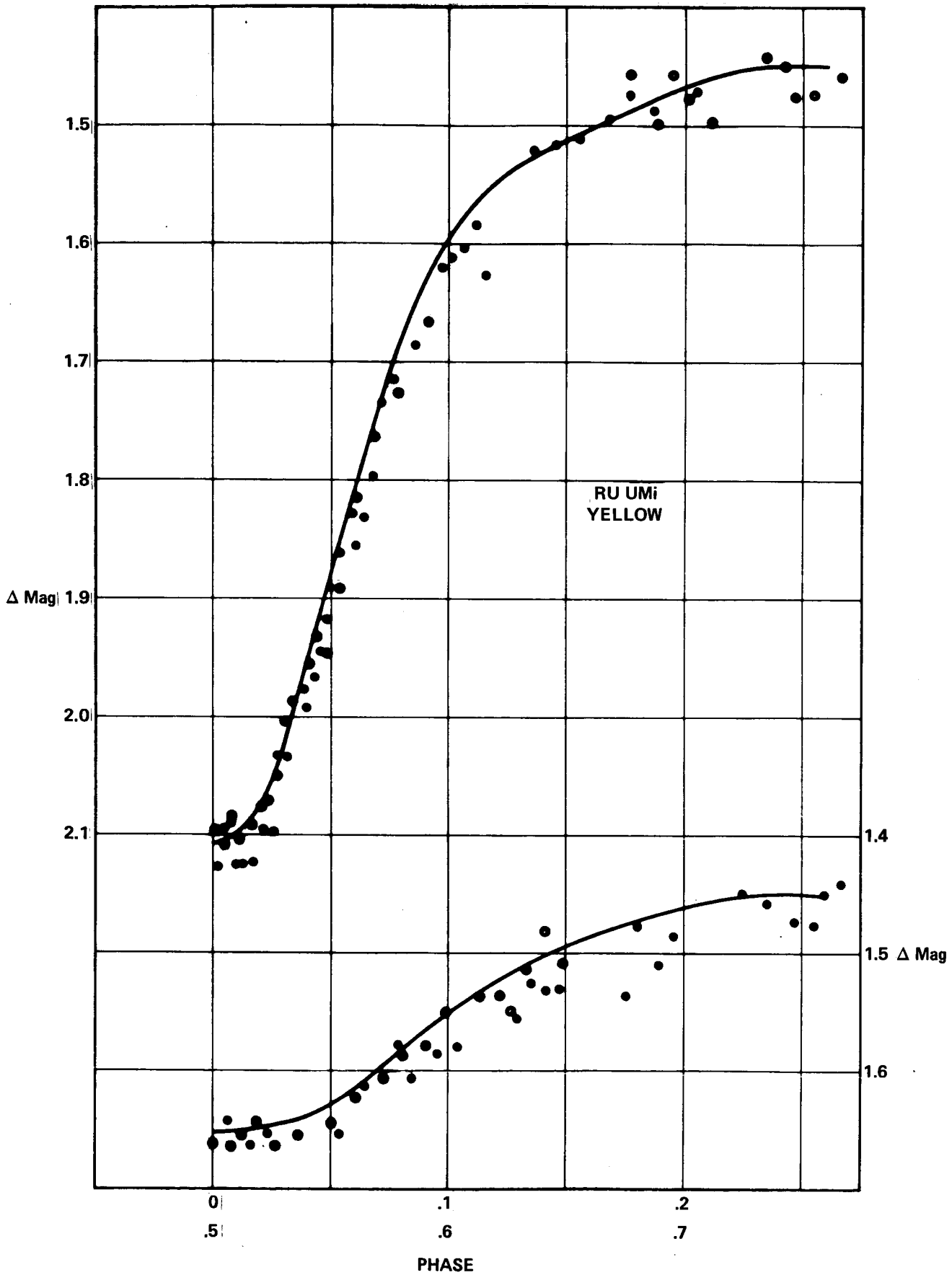

FIGURE 3 - FIT TO MODEL SOLUTION TO REFLECTED YELLOW NORMAL POINTS. THE OPEN CIRCLES ARE REFLECTED ABOUT MID-ECLIPSE

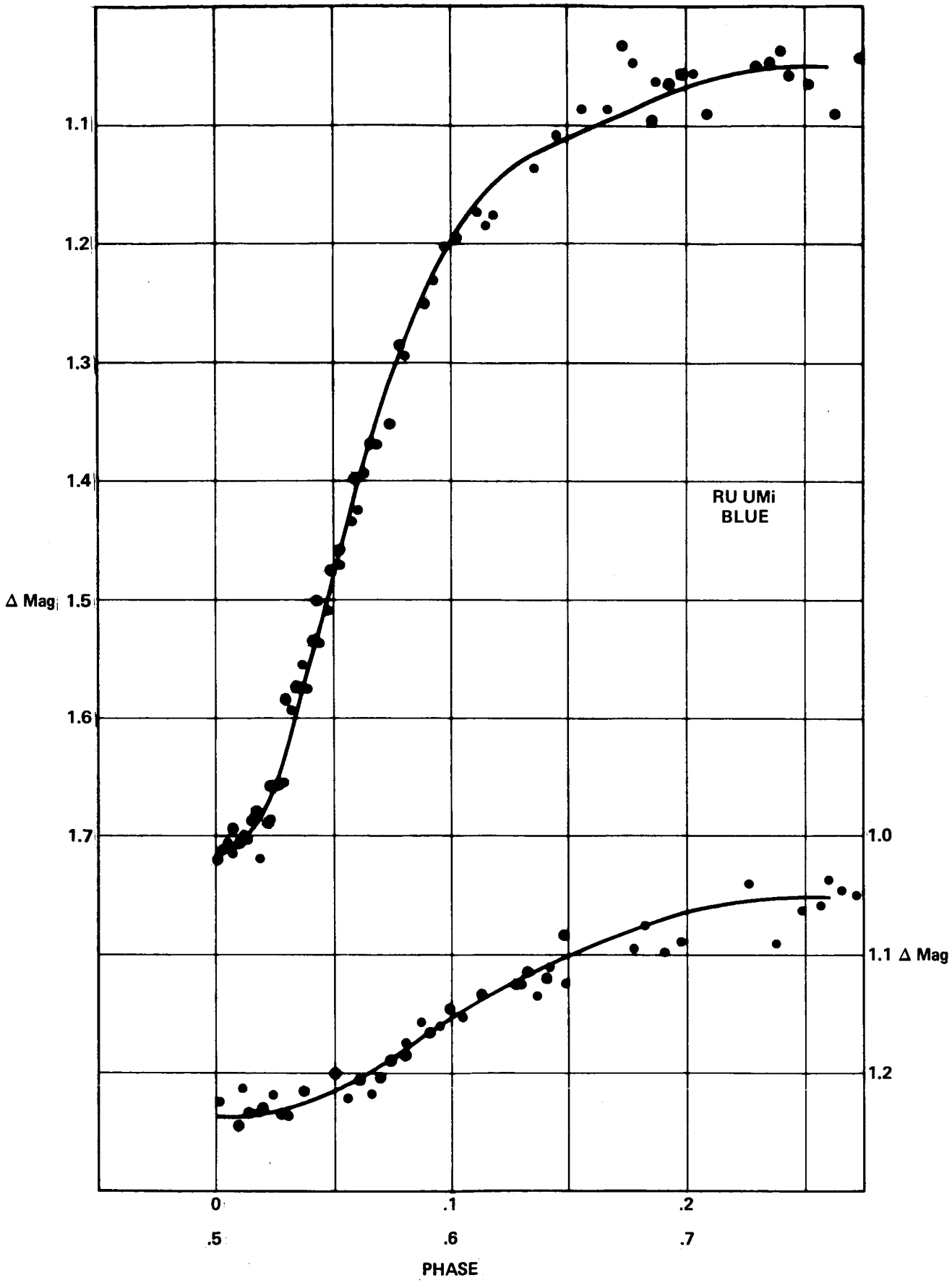

FIGURE 4 - FIT OF MODEL SOLUTION TO REFLECTED BLUE NORMAL POINTS

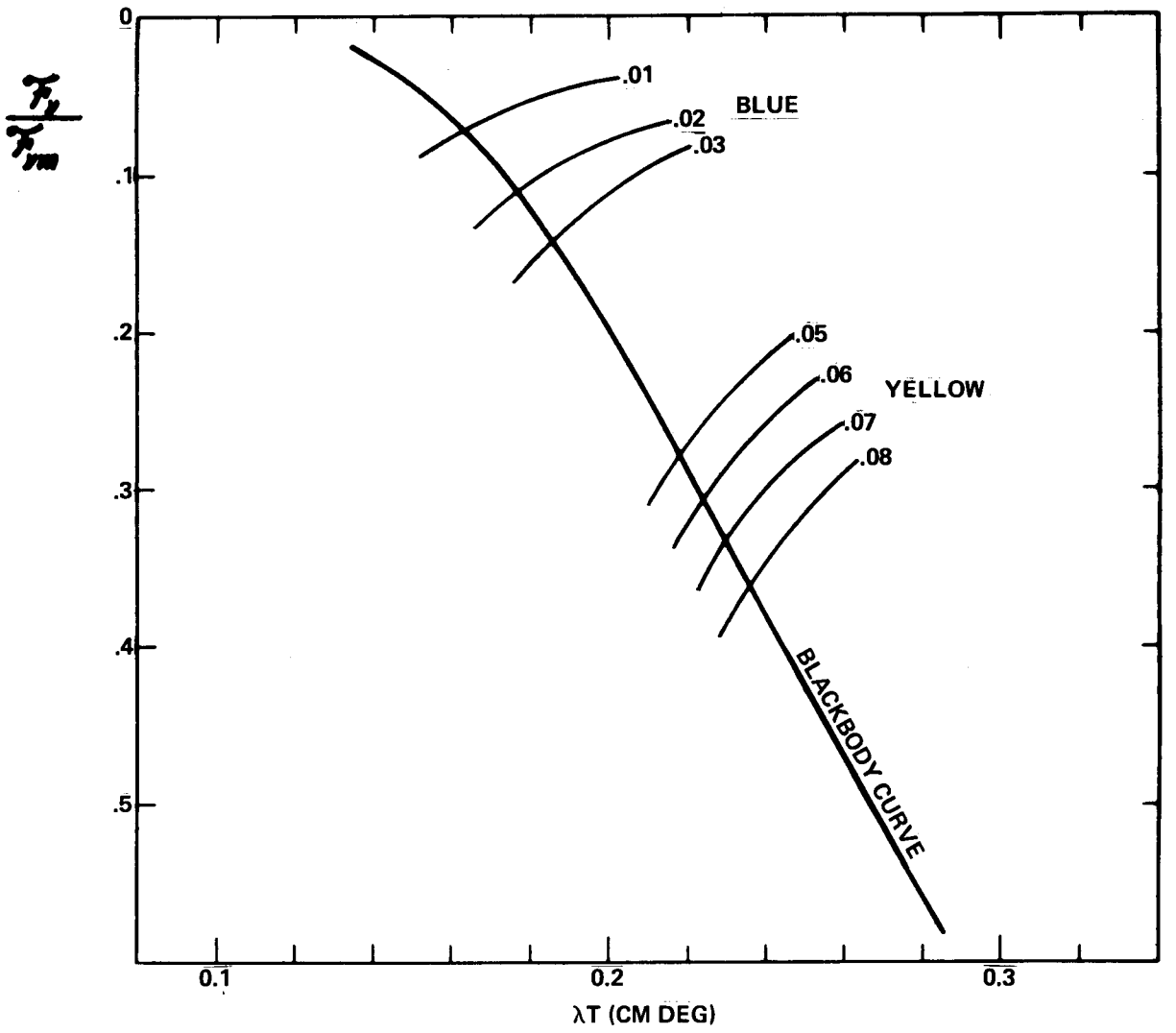

FIGURE 5 - FLUX AS A FUNCTION OF λT FOR BLACK BODY AND FOR VARIOUS RU UMi SOLUTIONS. CURVE SEGMENTS ARE LABELED WITH VALUE OF SURFACE INTENSITY RATIO, j, FOR YELLOW AND BLUE OBSERVATIONS

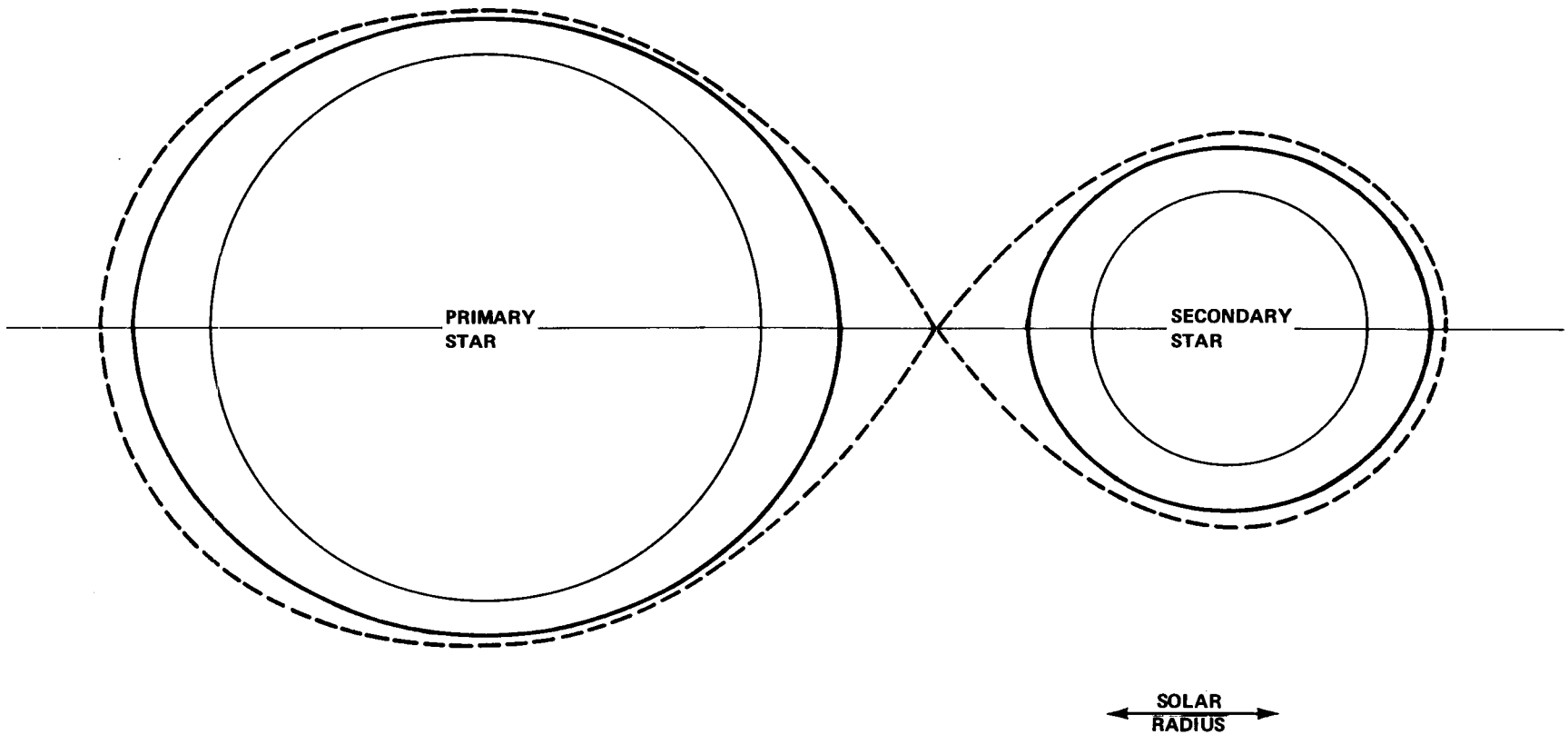

FIGURE 6 - SCALE DRAWING OF RU UMi AT QUADRATURE, AS SEEN BY A NEARBY OBSERVER LOCATED IN THE ORBITAL PLANE